

 Very Important Paper

Less is More: A Comprehensive Study on the Effects of the Number of Gas Diffusion Layers on Air–Cathode Microbial Fuel Cells

Pilar Sánchez-Peña,^[a] Jesús Rodríguez,^[b] Raquel Montes,^[a] Juan Antonio Baeza,^{*,[a]} David Gabriel,^[a] Mireia Baeza,^[c] and Albert Guisasola^[a]

Air-cathode microbial fuel cells (AC-MFC) use a gas-diffusion-layer (GDL) coating based on polytetrafluoroethylene applied to the cathode to prevent electrolyte leakage. However, this type of GDL can also lead to a decrease in MFC performance due to electron-transfer limitation, mass-transfer limitation or catalyst availability. This study provides a comprehensive understanding of the significance of the GDL coating, demonstrating the interaction between the number of GDL coatings and the external resistance (R_{ext}) used. An experimental design in 28 mL AC-MFCs was prepared and conducted using two different R_{ext} (10 and 249 Ω) and four different GDL coatings (1 to 4 layers). The coating effect was not significant when operating with a high R_{ext} where the electron transfer was the limiting process. However, when the R_{ext} was low, the amount of polytetrafluoroethylene limited the cathode performance due to a significant

decrease in the Pt availability on the catalytic surface. Thus, GDL-1 with 10 Ω as R_{ext} reached 0.96 mA/cm², 3-fold higher than that obtained with 249 Ω as R_{ext} (ca. 0.30 mA/cm²). Besides, the current density did not vary noticeably in the other cathodes with 249 Ω as R_{ext} . Contrarily, the current density with 10 Ω as R_{ext} decreased as the number of GDL increased (0.74, 0.57 and 0.37 for GDL-2, GDL-3 and GDL-4 respectively). These values agreed with those of the polarization curve. Furthermore, limitations were also observed in electrochemical impedance spectroscopy measurements: the charge resistance increased with the number of GDL, related to the ease of electron flow. These values were 18 Ω , 22 Ω , 53 Ω and 58 Ω for GDL-1, GDL-2, GDL-3 and GDL-4, respectively, for both 10 and 249 Ω cathodes.

1. Introduction


Searching for technologies that produce renewable energy from our wastes is critical in the current frame of adopting a circular economy. One of the most promising and emerging technologies is the use of Bioelectrochemical Systems (BES) also known as Microbial Electrochemical Technologies (MET). BES have been widely studied and are a current focus of interest because they can provide energy-efficient wastewater treatment, seawater desalination, renewable energy, and added-value chemicals.


BES combine electrochemistry with biological processes: enzymes or microorganisms act as a catalyst on one or both electrodes to oxidize and/or reduce undesired pollutants, to generate electrical energy, or to produce added-value products.^[1] BES rely on a group of microorganisms that have the ability to donate or accept electrons to/from a solid electrode that acts as a final electron acceptor or donor in the redox scenario. When these microorganisms are placed in the anode, they can oxidize organic matter using the electrode as the final electron acceptor.^[2] These microorganisms are known as exoelectrogens or anode respiring bacteria (ARB). Once oxidation reactions take place in the bioanode, which correspond with the oxidation of organic matter catalyzed by microorganisms (equation 1), the electrons travel from the anode to the cathode where an oxygen reduction reaction occurs (equation 2). There is a wide range of cathodic biological/chemical half-reactions that can occur in the cathode. Depending on the nature of the cathodic reaction, the whole cell will have a negative or a positive Gibbs free energy and therefore, the flow of electrons from the anode to the cathode will be spontaneous or not. The cell with a positive potential and, thus, a negative Gibbs free energy, will result in a spontaneous flow of electrons. These devices are known as microbial fuel cells (MFCs).^[3]

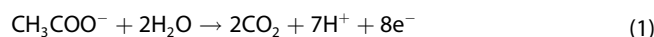
[a] P. Sánchez-Peña, Dr. R. Montes, Prof. J. A. Baeza, Prof. D. Gabriel, Dr. A. Guisasola
GENOCOV, Department of Chemical, Biological and Environmental Engineering, School of Engineering
Universitat Autònoma de Barcelona
Bellaterra, Spain
E-mail: JuanAntonio.Baeza@uab.cat

[b] Dr. J. Rodríguez
National Hydrogen Centre, Puertollano, Spain

[c] Dr. M. Baeza
Department of Chemistry, Faculty of Science, C-North building, Universitat Autònoma de Barcelona, Bellaterra, Spain

 Supporting information for this article is available on the WWW under <https://doi.org/10.1002/celec.202100908>

 © 2021 The Authors. ChemElectroChem published by Wiley-VCH GmbH. This is an open access article under the terms of the Creative Commons Attribution License, which permits use, distribution and reproduction in any medium, provided the original work is properly cited.





Thus, MFCs are devices that are able to generate electricity from organic matter oxidation by using ARB metabolism. These electrodes can be found in the same chamber or in two different chambers separated by an ion-exchange membrane (IEM).^[4] The electrons are transported through the external circuit,^[5] while the charge balance is obtained through the transport of ions such as protons and hydroxyls through the membrane. The electrons react with the oxygen present in the cathode, resulting in water formation.^[6]

An MFC configuration integrates well the circular economy concept when wastewaters containing organic carbon are oxidized in the anode to generate electricity from that waste. The objective of an MFC treating wastewater is to create a high anodic oxidation rate of organic matter and, consequently, a high flow of electrons from the anode to the cathode, *i.e.* to produce a high current^[7] that would lead to high power in addition to wastewater oxidation. Several authors have studied the factors that can increase the power of an MFC such as the microbial inoculum, the internal and external cell resistances, the ionic strength of the culture medium and the electrode materials.^[8,9]

Among them, electrode materials have become a key factor to increase electricity generation, since oxidation and reduction reactions take place on the electrodes. The cathode material has received much more attention as it is commonly accepted as the limiting step in MFC performance due to the poor oxygen reduction kinetics.^[10–12]

Amidst the different MFC configurations, the air-cathode (AC-MFC) is the most preferred. The cathodic chamber is directly open to the air through a cathodic electrode, which allows oxygen to diffuse through it. This configuration is the most likely configuration to be scaled up due to its simple structure, high power output, and relatively low cost.^[13]

Despite its apparent simplicity, the air-cathode architecture becomes critical for MFCs performance.^[14] It is formed by two well-defined zones: a hydrophilic zone, in contact with the electrolyte, and a hydrophobic one that faces the atmosphere. These zones do not coincide exactly with catalyst and gas diffusion layers, but a gradient of both along the cathode is required to create a triple-phase interface where the simultaneous interaction between protons (liquid phase), oxygen (gas phase) and electrons (solid phase) occurs.^[15] In fact, an unbalanced gradient could present high hydrophilicity or hydrophobicity, causing a limitation on protons transport or a flooding phenomenon, respectively.^[16]

Therefore, the importance of a proper design and structure of each cathode seems evident. In this sense, the Gas Diffusion Layer (GDL) plays a fundamental dual role. On the one hand, it allows oxygen diffusion so that oxygen reduction is conducted at the inner layer with the highest oxygen concentration possible. On the other hand, GDL has to avoid culture medium leakage (Figure 1a). Gas diffusion layers made of polytetrafluoroethylene (PTFE) can meet both requirements^[17] among other hydrophobic polymers,^[14] at the expense of increased

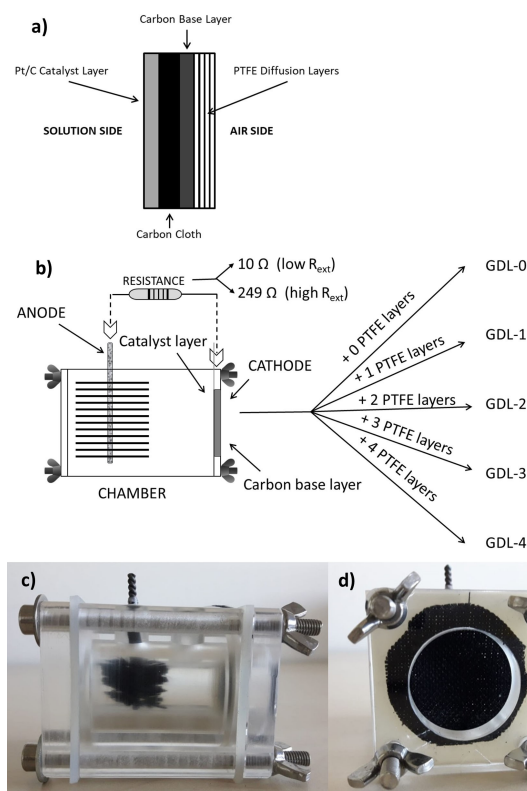


Figure 1. Description of the AC-MFCs used in this study: a) Side-view of a cathode with four gas diffusion layers (GDL-4), b) schematic, c) side picture showing the graphite fiber brush anode and d) front picture showing the carbon cloth cathode.

internal resistance (R_{int}) as PTFE is non-conductive and thus it may hinder the AC-MFC performance. GDL are built by painting the electrode, usually carbon cloth, with PTFE as many times as layers are desired. In previous works, it was found that the optimal number of PTFE layers was four,^[18] although with fewer layers, the start-up of MFCs was faster and a higher current output was achieved.^[14]

Therefore, a better understanding of the effects of the number of GDL coatings is essential to improve oxygen diffusion without leading to cell leakage. GDL have received a certain attention^[19–22] but, in general, the fact that these layers can limit the performance of an AC-MFC has not been deeply addressed, even though they could have an impact for certain processes. Li et al.^[23] observed that the presence of GDL had a higher influence on the charge transfer resistance than the catalyst layer for single chamber AC-MFCs. Santoro et al.^[20] found that the deposition of several PTFE layers in the air-facing side of the cathode could reduce the pore size, which increased the electrode resistance and hindered oxygen diffusion to the catalyst layer.

Besides that, oxygen reduction (reaction 2) has slow kinetics and, hence, the cathode needs a catalyst layer, which is in contact with the culture medium. The most commonly used catalyst is platinum (Pt).^[24] The use of Pt for large scale MFC may be hindered by its high price, so, several alternatives are

currently being sought.^[25,26] However, at this stage, Pt is still the most used catalyst in lab-scale MFC configurations.

This work aims to better understand the overall effects of the number of GDL coatings and external resistance (R_{ext}) on AC-MFC performance. For this purpose, several AC-MFCs were built with cathodes based on carbon cloth and different number of GDL coatings to study its effect. Furthermore, two R_{ext} were tested to study the effect on the performance of the MFCs: 1) a high R_{ext} (249 Ω) as the most widely used^[27] and 2) a low R_{ext} (10 Ω). Although the influence of the number of catalyst layers has been previously addressed by different authors, commonly reported studies have only focused on high external resistances, i.e. at medium-low current density. However, the low resistance section is frequently ignored. At high currents, different interesting phenomena occur (mass transfer limitations, maximum current density, etc.). The evaluation of the behavior of air-cathodes with different number of GDLs under these conditions could make other phenomena visible, providing valuable information on the influence of this component on the cathode performance. To the best of the authors' knowledge, the combined influence of GDL coatings and current density on MFC performance has not been reported previously. Thus, the present approach represents a novel contribution to a better understanding of the influence of GDL on the performance of air-cathodes in MFCs. The performance of the MFCs was assessed using a bioanode to reach more realistic conditions. Different electrochemical techniques like Electrochemical Impedance Spectroscopy (EIS), polarization curves and Cyclic Voltammetry (CV), and optical microscopy techniques like Scanning Electron Microscopy (SEM), Energy Dispersive X-Ray (EDX) and Brunauer-Emmett-Teller (BET) surface area analysis, have been used to assess the electrochemical characteristics and behavior of the MFC.

2. Results and Discussion

Firstly, the effect of the number of GDL coatings on the cathode morphology and the AC-MFCs performance was studied by SEM. The overall oxygen mass transfer coefficient was also determined to evaluate the effect of GDL over oxygen diffusion. Then, the performance of MFCs with different GDL cathodes was assessed using several bio/electrochemical techniques.

2.1 Characteristics of the Cathode

The cathode surface was characterized without the presence of microorganisms. SEM images were taken (Figure 2) for cathodes with a different number of GDL coating (GDL-0 to GDL-4). The individual carbon fibers could be distinguished when no coating was applied (GDL-0). A high porosity of the carbon fibers was observed, which is theoretically beneficial since it results in a large active area, which would lead to a high current density. However, these large pores also caused a high leakage of culture medium (average value of 20 mL per week).

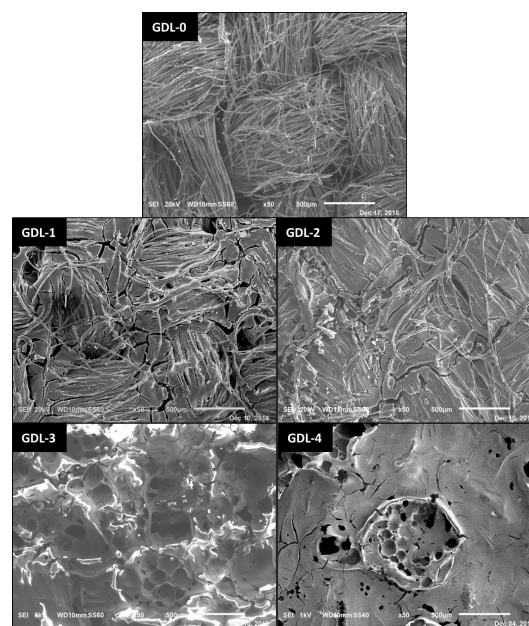


Figure 2. SEM images corresponding to carbon cloth with a different number of GDL coating (GDL-0 to GDL-4).

Consequently, AC-MFCs using this type of GDL-0 cathode were discarded.

A homogeneous PTFE layer with many cracks over the carbon fibers could be observed for the one diffusion layer cathode (GDL-1). A similar morphology was observed for the two diffusion layers cathode (GDL-2), while GDL-3 showed fewer cracks and a very irregular surface where carbon fibers could not be clearly distinguished. GDL-4 was the cathode tested with the highest amount of PTFE, showing a less rough surface where no fibers nor cracks could be observed either. So as to analyze the specific surface area for each cathode, BET (S_{BET}) was measured (Table 1). A reduction of the S_{BET} and of the pore volume was found when increasing the number of GDL. The application of more PTFE layers progressively covered the surface of the fibers. Thus, the accumulation of PTFE would potentially lead to a negative effect on cell performance due to a reduction of the specific surface area available. In addition, the more GDL added, the more PTFE was deposited. Figure S1 compares a SEM image of a cathode with one and four PTFE layers and indicates the pore occupation. Moreover, PTFE is a non-conductive material and, thus, its accumulation would lead

Table 1. Specific surface area (S_{BET}), pores volume, oxygen diffusion coefficient (D_{O}), and thickness (δ) obtained for cells with GDL-0, GDL-1, GDL-2, GDL-3 and GDL-4.

GDL	S_{BET} [$\text{m}^2 \cdot \text{g}^{-1}$]	Pores volume [$\text{cm}^3 \cdot \text{g}^{-1}$]	D_{O} [$\text{cm}^2 \cdot \text{s}^{-1}$]	δ [μm]
GDL-0	1.171	0.0045	ND ^[a]	658
GDL-1	0.724	0.0033	$5.37 \cdot 10^{-4} \pm 2.4 \cdot 10^{-5}$	623
GDL-2	0.582	0.0028	$4.17 \cdot 10^{-4} \pm 1.3 \cdot 10^{-5}$	600
GDL-3	0.486	0.0021	$3.63 \cdot 10^{-4} \pm 1.9 \cdot 10^{-5}$	615
GDL-4	0.417	0.0020	$2.80 \cdot 10^{-4} \pm 2.1 \cdot 10^{-5}$	616

^[a]ND: not determined.

to a higher internal resistance and, thus, to a lower performance.

Besides that, the pore volume is directly related to the amount of oxygen that can enter the cell through the cathode. The oxygen diffusion coefficients (D_{O_2}) of each cell were calculated according to equation (5). Table 1 shows that D_{O_2} decreased as the number of GDL increased. A too high number of GDL would end up producing a limitation due to a reduced oxygen diffusion. Moreover, according to Fick's law, the oxygen flux is also dependent on the thickness of the solid. The thickness of the cathodes (δ) with and without GDL was measured also through SEM (Figure S2 and Table 1). No direct correspondence was found between the number of GDL and the total cathode thickness. While the GDL-0 had the maximum thickness and the thickness decreased for GDL-1 and GDL-2, an increase was found for GDL-3 and GDL-4. The lack of correlation between the number of GDL and the thickness was due to the PTFE role as a binder that compacted the electrode for GDL-1 and GDL-2 while filling the pores. However, PTFE accumulated in the surface when all the pores were filled and resulted in an increased thickness for GDL-3 and GDL-4. Consequently, it does not seem accurate to classify a cathode by its thickness when the standard procedure for building air-cathodes^[21] is used. Interestingly, the ratio between the D_{O_2}/δ , i.e. K_L , showed almost 2-fold higher value for GDL-1 compared to GDL-2, GDL-3 and GDL-4 (Table 1), indicating that the correlation of higher oxygen limitations as the number of GDL raised was more significant for $GDL > 2$.

The thickness and porosity of the cathodes have been extensively studied. It is worth mentioning that there are other techniques to manufacture cathodes and to control the porosity.^[28] Oppositely, it has been studied that these parameters can vary depending on many factors, such as the carbon material support^[29] or even the polymer binder and the fabrication method.^[30] Therefore, the deposition of the different number of GDL is not the only factor to be determined in the study of thickness and porosity.

A reduction of the GDL increases the surface area, reduces the internal resistance (R_{int}) and, thus, enhances the cell performance. However, the availability of the catalyst is a parameter that needs to be considered and it depends on its distribution over the cathode and, thus, on the number of GDL coatings. Understanding the catalyst distribution in the cathode is necessary when aiming at scaling up MFCs. The conventional catalysts used in MFCs are often expensive. When using metals, such as Pt, minimizing the amount of Pt dosed and maximizing its accessibility is essential in view of decreasing cell manufacturing costs. Pt must be accessible and exposed to the catholyte to maximize its catalytic activity. Thus, Pt must be located as close as possible to the inner layer of the cathode surface in contact with the catholyte. Cross-sections of cathodes using SEM-EDX images provided information about the metal distribution in the cathode. Figure 3 shows the cross-section of the GDL-4 cathode while Figure S3 provides the SEM images of cross-sections of cathodes from 0 to 4 GDL, which confirms that the different layers were applied correctly. The right side in each picture corresponds to the external surface of the cathode

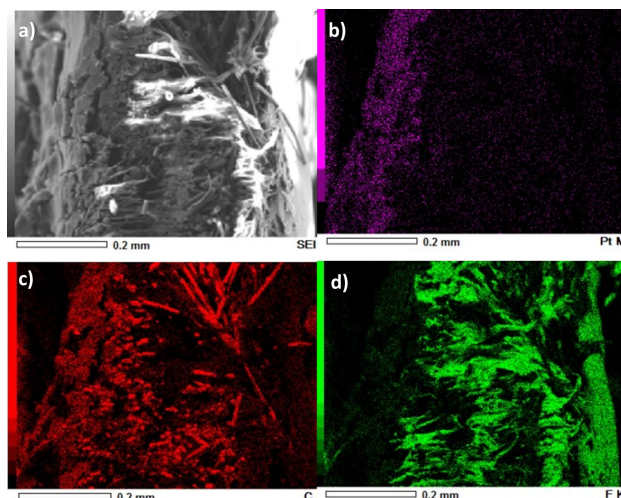


Figure 3. SEM Mapping of a cross-section cathode with GDL-4. This figure shows a) SEM cross-section of the cathode. EDX mapping for b) Pt, c) Carbon, d) Fluorine.

(in contact with air) while the left side corresponds to its internal surface (in contact with the catholyte). Figure 3a shows a cross-section of the cathode using SEM where the fibers of the cathode can be observed. Since SEM images were taken in perspective, blue arrows are used to help visualize the thickness of the cathode. Such a structure was further visualized with EDX (Figure 3b and 3c) and fluorine (Figure 3d) spectra. Figure 3b shows the Pt in the EDX spectra, demonstrating that Pt accumulated in a very homogeneous and thick layer on the internal side of the cathode. Figure 3c shows the carbon (C) in the EDX spectra. As expected, C was found to be distributed in the whole cathode because the material was carbon cloth and the catalyst ink contained 90% C and 10% Pt. Since PTFE contains fluorine, the fluorine spectra (Figure 3d) showed that the GDL was located mainly on the external side of the cathode and confirmed the penetration of PTFE in the pores of the carbon cloth.

Figure S1 provides an idea of the penetration degree of PTFE in the carbon cloth for GDL1 and GDL4 (without catalyst layers). Red circles evidence how increasing the number of PTFE layers will translate into a deeper PTFE penetration. While the thickness of PTFE layer was constant in GDL1, it varied in GDL4 since the PTFE adapted to the morphology of carbon cloth. The presence of F in the catalyst layer was related to the small amount of Nafion that was used in the catalytic ink. A comparison of the fluorine and the EDX spectra for Pt of a cross-section of cathodes with a different number of GDL coating (Figure S3) showed a reciprocal relation between the number of GDL and the Pt availability.

The electroactive surface was analyzed through CVs with a solution containing iron (III) and iron (II) to evaluate the amount of active Pt on the cathode surface. Two peaks appeared that corresponded to the iron oxidation and reduction. The intensity of the current peaks was proportional to the electroactive surface area according to the Randles-Ševčík equation (equation 7). The obtained electroactive surface area values were

2.15, 1.86, 1.31 and 1.14 cm² for GDL-1, GDL-2, GDL-3 and GDL-4, respectively. These values confirmed a higher Pt availability when the electrode had a lower amount of PTFE. Thus, an increasing number of GDL leads to a higher blockage of the pores due to the PTFE coating and penetration (Figure S1 and S3) that leads to a reduced amount of Pt available that preferentially distributes closer to the inner surface of the cathode, *i.e.* there is less Pt available as catalyst. Furthermore, the difference in electroactive area between GDL-2 and GDL-3 was 42 %, a higher value compared with the difference between GDL-1 and GDL-2 (15 %) and GDL-3 and GDL-4 (15 %).

2.2 Evaluation of Power Generation as a Function of Circuit Resistance

The performance of the MFCs with different GDL coatings was assessed using polarization and potential curves (Figure 4). Polarization curves (Figure 4a) can be divided into three well-defined zones.^[31] In the range of low current density (between 0 and 0.05 mA/cm²), the potential sharply decreased due to the activation overpotential. The response between 0.05 and 0.3 mA/cm² became linear because the ohmic overpotential prevailed over the overpotentials at the cathode and the anode.

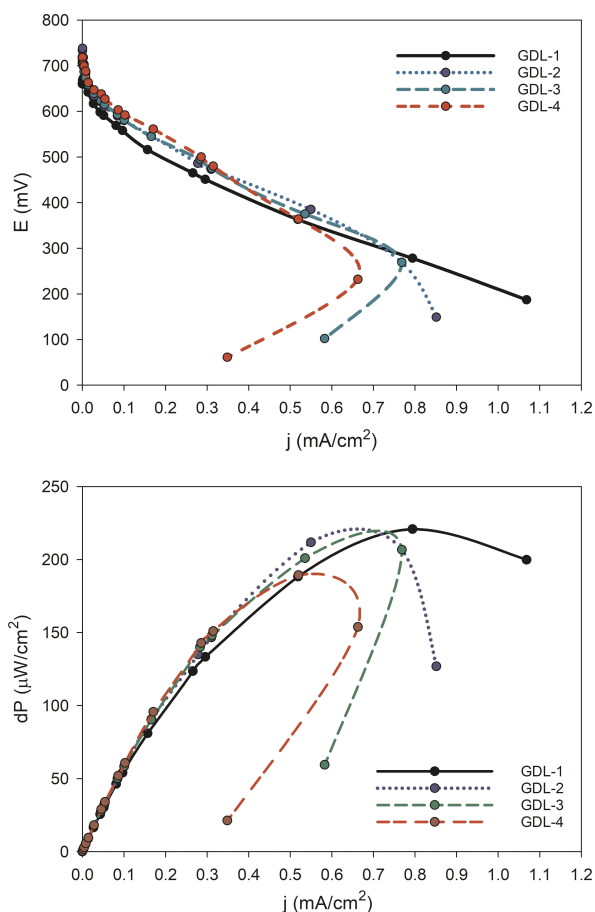


Figure 4. Polarization curve of different cathodes with different number of GDL (GDL-1 to GDL-4). a) Polarization curve and b) power curve.

The behavior of the cells in these two regions was very similar regardless of the number of GDL. Thus, under the same operational conditions, all the cells showed a similar behavior. On the contrary, at higher current densities, *i.e.* when the potential was lower than 280 mV, each cell showed a different response. Figure 4b shows that the power density curves also have a common region for all MFCs. Similar maximum power densities of around 130 µW/cm² were obtained for GDL-1, GDL-2 and GDL-3. At high R_{ext} (around 470 kΩ), the limiting factor was the charge transfer, and therefore, the power density obtained was similar. However, Figure 4b shows that under low resistance (25 Ω), the current density decreased when the number of GDL coating was higher, decreasing for GDL-4 down to 29 % of that of GDL-1 (from 1.1 mA/cm² to 0.32 mA/cm²).

Thus, figures 4a and 4b show that the current density decreased when low R_{ext} was used for cathodes with a higher number of GDL. The underlying causes of this phenomenon, known as power overshoot,^[32–34] have not been fully elucidated yet but attributed to different factors. The most accepted hypotheses are:^[33] (i) The microbial biofilm has an inability to produce higher current densities or to respond to the elevated anode potentials, *i.e.* when the R_{ext} is low, the bacteria on the anode cannot produce sufficient current at lower voltages, (ii) the sampling time is too fast and the anodic community does not have time to acclimate to new anode potentials, (iii) there is a limitation of the reactants, in this case acetate in the anode or oxygen in the cathode, and (iv) a toxic has reduced the cell performance.

Given the characteristics of our experiments, the different response at low R_{ext} is due to a limitation in the reactants and that raises two different hypotheses: 1) the limiting factor could be the amount of available Pt, which depends on the number of GDL coatings, and 2) the limiting factor would be the mass transfer limitation (specifically oxygen diffusion) due to the width of the GDL. The first hypothesis would support the argument that the amount of available Pt would limit the cell performance rather than the charge transfer at high current density. As a result, less oxygen would reach the catalyst active sites and the efficiency of the entire process would be reduced. Consequently, the overpotential would become higher, generating a lower current density. This would not be observed in the GDL-1 AC-MFC since the amount of Pt available was larger because the pores were not blocked with PTFE and they could be occupied by Pt. On the other hand, the second hypothesis would support the argument that the reactant demand was higher than the reactant availability at the cathode. In other words, mass transfer would be limiting cell performance rather than charge transfer. However, in the GDL-1, the oxygen diffusion would be so favored that it did not limit the cell performance, reaching the highest current density. Thus, both hypotheses sustain that the cell performance was less limited at high current densities in GDL-1. In fact, 1.07 mA/cm² was obtained for GDL-1 while 0.85, 0.77 and 0.66 mA/cm² were obtained for GDL-2, GDL-3, and GDL-4, respectively. Thus, the polarization curve provides information about the limiting factor at low and high R_{ext} , being charge transfer limitation at

high R_{ext} and Pt availability or mass transfer limitation at low R_{ext} .

On the other hand, the MFCs performance herein was enhanced compared to the results reported using other binders. For instance, a MFC with a spun-bonded olefin diffusion layer^[35] instead of GDL with PTFE showed 47% less power density comparing with GDL-4 cathode and 73% worse comparing with a GDL-1 cathode. The use of carbonized kraft paper as support instead of PTFE^[36] resulted in MFCs with 33% less power comparing with a GDL-4 cathode and 57% more using a GDL-1 cathode. It could be because PTFE is a liquid that, when it is deposited and dried, adopts the shape of the electrode. Oppositely, spun-bonded olefin and kraft paper are usually more rigid, providing less relief and less contact area, thus, electrodes with similar projected surface area (~4 cm diameter) showed a worst performance.^[36]

2.3 Monitoring of the Current Density Generated from Acetate

Current density generated from acetate was monitored with the purpose of deeply studying the limiting factors of MFCs. Acetate-fed MFCs with cathodes with different GDL coatings were operated for more than three months under different R_{ext} (249 and 10 Ω , Figures 5a and 5b, respectively) without any performance decay being detected during this period. Figure 5a shows the current density evolution of cells with different GDL at a R_{ext} of 249 Ω . Results showed a similar response (less than 7% of error) for all MFCs, reaching almost the same maximum current density. This behavior agreed with the first zone of the polarization curves (Fig 4a). Under these conditions, the process was limited by electron transfer because the MFC was externally connected to a high resistance. Thus, the electrons flow was slower, thereby limiting the charge transfer on the electrodes. The coating of the GDL did not influence the performance of the cells and the amount of reagent (*i.e.* oxygen) that reached the active centers of the cathode was not limiting compared with charge transfer processes. Thus, a better performance, *i.e.* higher current density, is expected in cells with lower R_{ext} based on Figure 4.

On the contrary, MFCs with lower R_{ext} (10 Ω) showed a different response to the different number of GDL coating (Figure 5b). In this case, the electron flow was facilitated due to the low resistance, allowing electrons to easily reach the cathode. Consequently, the electrochemical response was limited by one of the above-mentioned hypotheses: 1) by the number of active sites in the cathode able to catalyze oxygen reduction, *i.e.* by Pt availability, or 2) by mass transfer, *i.e.* the amount of oxygen in the cell. Figure 5b shows that the higher the number of GDL coating, the lower the response of the cell because of the lower Pt or oxygen availability in the cathode. Accordingly, the maximum current densities obtained were (mA/cm^2): 0.96, 0.74, 0.57 and 0.37 for GDL-1, GDL-2, GDL-3 and GDL-4, respectively. These trends were in good agreement with current density values under high current intensity in the polarization curves (see Figure 4).

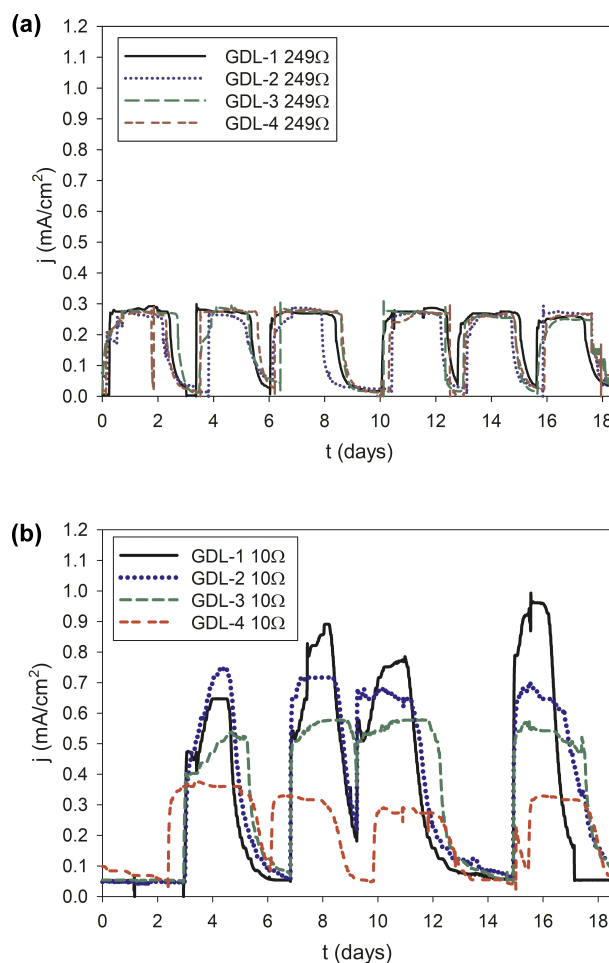


Figure 5. Current density obtained for selected cells when the R_{ext} was 249 Ω (a) and 10 Ω (b). Both replicates of each GDL cell provided similar results.

The GDL-1 cell showed a variable maximum current density response for each cycle (from 0.72 to 0.96 mA/cm^2). These variations were attributed to culture medium leakage through the cathode (due to the high porosity of carbon cloth) because in each cycle part of the culture medium had to be renewed, but the leakage per cycle was lower than 10% of the total volume of the cell, so the cell continued working. Hence, catholyte leakage was observed when the GDL was not thick enough.

2.4 Coulombic Efficiency (CE)

CE stands for the percentual ratio of the coulombs recovered as current intensity to the theoretical coulombs generated from substrate oxidation (equation 8). Figure 6 shows CE for the cells with different GDL coating at low and high resistances. On the one hand, the CE in MFCs with low R_{ext} progressively decreased when the number of GDL increased (CE closed to 100% for GDL-1 whereas CE was lower than 60% for GDL-4). According to the electroactive area results, a lower number of GDL coating

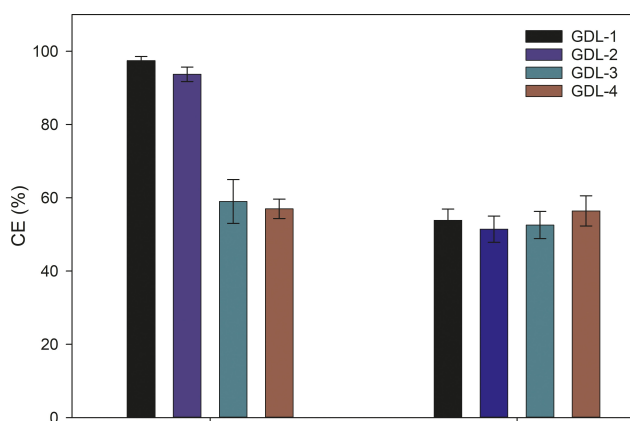


Figure 6. CE for cathodes with different number of GDL. Mean value for each cell with error bars indicating the range of values.

leads to a larger cathodic specific surface area with a higher Pt availability and higher oxygen penetration.

If an oxygen limitation was the cause of the current densities at low R_{ext} ,^[18] the CE would not have decreased as the number of GDL coatings increased. If Pt is not limiting and oxygen is the limit, all the entering oxygen would be electrochemically reduced at the surface catalyst and the CE values should not be affected by the number of coatings. However, our results show that CE increased when decreasing the number of GDL coatings. A limitation in Pt availability can describe the observed results. When the number of GDL is low, the CE is high since all the oxygen intrusion is reduced electrochemically by the Pt. However, when the number of GDL is higher, the Pt availability is hindered and part of the oxygen can be diverted to biological aerobic processes (such as heterotrophic acetate oxidation) and the CE would decrease. In this scenario, the lower the amount of GDL, the higher the CE due to the higher availability of Pt for catalysis.

Therefore, the hypothesis of oxygen transfer limitation was discarded. On the other hand, Figure 6 also shows that when R_{ext} was 249 Ω all MFCs obtained similar CEs (around 50–55%). This lack of effect of the number of GDL in the CE indicates that for the high R_{ext} of 249 Ω , the cell performance and the electrochemical parameters showed low variations because the limiting factor was the electron transfer.

Other authors operating at 100 Ω as R_{ext} noted that the CE increased when the number of GDL increased and, consequently, the hydrophobic treatment of cathodes was boosted.^[37] They attributed this observation to the fact that oxygen permeation to the catalyst layer was reduced and the conversion of organic substrates to electricity was enhanced. In any case, the different trends observed for each specific study greatly depend on the operational conditions and performance for the MFCs, such as anode activity, specific cell geometry, external resistance, catalyst availability and other factors.

Nevertheless, the CE values obtained in our study confirmed that the limiting factor of our system at low R_{ext} was the Pt availability while at high R_{ext} it was the electron transfer.

2.5 Analysis of the Electrodes using Electrochemical Impedance Spectroscopy

EIS measurements were performed in cells inoculated at R_{ext} of 10 and 249 Ω . Figure 7 shows the Nyquist diagrams for 10 Ω cells for cathodes with a different number of GDL coating. The circuit used (Figure 7) was the well-known simplified Randles circuit, *i.e.* without the Warburg element,^[38] where R_s is the ohmic resistance, associated to electrolyte and components resistance (electrode, membranes...), R_{ct} is the charge resistance, related to the ease of the electron flow and therefore, with the electrochemical reaction on the cathode surface, and C_{dl} is the capacitance, associated with the double electrolytic layer.

Table 2 reports the cell resistances of the equivalent circuit fitted to the experimental EIS measurements. The R_s values for 10 and 249 Ω R_{ext} were roughly similar because the electrolyte was the same and the components were similar. It is true that the electrode was slightly different. Thus, when the number of GDL increased, the electrode became less conductive and for this reason, the general trend was that R_s increased. In any case, R_s has been suppressed in Figure 7 for a better understanding of the EIS plots. The R_{ct} was 300% higher with GDL-4 than with GDL-1 for both cases, indicating the strong effect of the number of GDL coatings on the conductivity of the electrodes and so, the electron flux. The observed trend was in good accordance with previous results: a higher number of layers increases the R_{ct} of the cell because the charge transfer in the cathode is

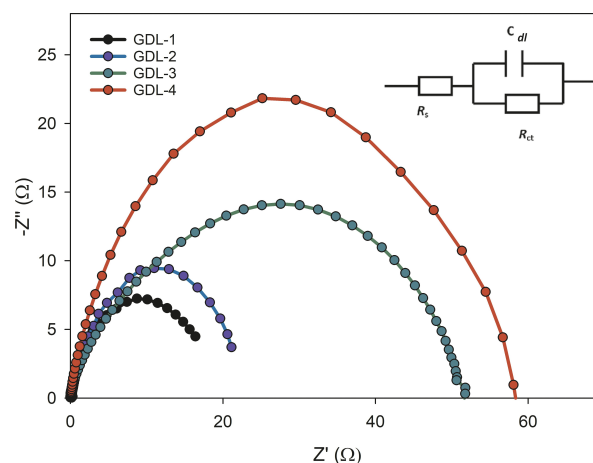


Figure 7. EIS results of AC-MFCs operated with 10 Ω R_{ext} and posteriorly fitted to the simplified Randles circuit: $R_s \cdot (R_{\text{ct}} \cdot C_{\text{dl}})$ (inset). Frequency range from 100 kHz to 10 mHz.

Table 2. MFCs resistance obtained in the simplified Randles equivalent circuit in MFCs inoculated at R_{ext} 10 and 249 Ω and different GDL

GDL	R_s [Ω] (10 Ω)	R_{ct} [Ω] (10 Ω)	R_s [Ω] (249 Ω)	R_{ct} [Ω] (249 Ω)
GDL-1	6.9	18.2	6.5	18.6
GDL-2	11.5	22.1	7.4	22.2
GDL-3	16.2	52.1	6.8	53.8
GDL-4	16.5	58.0	11.9	57.8

hindered and because of the lower Pt availability. Furthermore, this was also due to the thickness of the number of GDL, where it was previously observed that the thickness was not directly proportional to the number of GDL but to the resistance due to the accumulation of PTFE. The more layers of PTFE were deposited, the higher the observed R_{ct} .

Table 2 also shows that the cells can be grouped according to the R_{ct} values (GDL-1 and GDL-2 and cells with GDL-3 and GDL-4). This correlates with the electroactive area values shown in the section "Characteristics of the cathode", where the same grouping was observed. Thus, GDL-1 and GDL-2 had lower R_{ct} because there was a larger amount of Pt available.

Besides that, the R_s and R_{ct} were similar in cells with the same number of GDL, independently of the R_{ext} used. This suggests that, despite being a handmade method, the cathode production was very reproducible with similar cathodes obtained on different days.

3. Conclusion

After studying AC-MFCs with cathodes containing different number of GDL coatings (from GDL-0 to GDL-4), it was shown that the cell performance depends on the R_{ext} used (10 and 249 Ω). The AC-MFC limiting factor at high R_{ext} is the electron transfer and the cells have similar performance regardless of the number of GDL coatings. However, the number of GDL coatings at low R_{ext} is very significant: the Pt availability for catalysis becomes the main limiting factor when using a high number of GDL.

CE and EIS techniques were essential to understand this cell limitation. Lower CE values were observed when working with high R_{ext} for all GDL coatings and with low R_{ext} and 3–4 GDL. The results for low R_{ext} indicate that the lower CE was a consequence of the oxygen entering the cell being higher than the available oxygen reduction capacity, which was related to the Pt availability on the cathodic surface. In the case of high R_{ext} , the additional limitation of increased electrical resistance led to a lower oxygen reduction capacity for all tested GDL coatings. Furthermore, it could be observed through EIS that R_{ct} increased when the amount of GDL increased because the PTFE blocked the pores and decreased the amount of available Pt.

SEM images showed a higher porosity of the cathode surface and larger available surface area at low GDL, in accordance with the trend of S_{BET} values. Besides, as the number of GDL decreased, the amount of Pt available on the cathode surface increased because less PTFE blocked the pores on the cathode surface, making Pt availability higher, matching the electroactive area values.

Experimental Section

Microbial Fuel Cell Construction

The single-chamber AC-MFC (Figure 1b–d) consisted of a 28 mL cube cell made of methacrylate (4.4 cm length \times 5 cm width \times 5 cm

height), with a lateral aperture (3 cm diameter) where the cathode was located. It was assembled with two lateral methacrylate endplates, using O-rings and gaskets to prevent electrolyte leakages. These pieces were kept together by tightening screws and wing nuts.^[39]

Regarding the electrodes, the anode was a graphite fiber brush (2.0 \times 2.5 \times 5.0 cm) with a titanium wire, which worked as a current collector. It was thermally treated in a muffle furnace at 450 $^{\circ}$ C for at least 30 minutes to remove the impurities and to generate microfractures in view of increasing the active area and, thus, enhancing biomass adhesion.^[40]

On the other hand, the cathode (Figure 1a) was a 7 cm² carbon cloth layer (Carbonized Woven Fabric, Plain Weave, Zoltek) that was treated according to the following widely extended standard procedure.^[41] Firstly, a carbon-based layer was coated over the carbon cloth to increase the conductivity. This carbon-based layer consisted of a mixture of carbon black (1.56 mg/cm²) and 40% w/w PTFE solution (12 μ L/cm²) and was prepared by vortex agitation for 20 seconds. It was coated onto the carbon cloth using a paintbrush and then air-dried for 2 hours and heated at 370 $^{\circ}$ C for 30 minutes.

Afterwards, a GDL was added to the previously coated side. This layer consisted of painting with 60% w/w PTFE solution (Sigma-Aldrich) using a paintbrush. The coating was allowed to air-dry for at least 10 minutes, where the coating should turn white when dry, and then, heated at 370 $^{\circ}$ C for about 10 more minutes. This process was repeated between 1 and 4 times, depending on the desired GDL applications, yielding GDL labelled as GDL-1, GDL-2, GDL-3, and GDL-4. Additional cathodes without an externally applied GDL (GDL-0) were also tested. Figure 1b shows a schematic AC-MFC used with different cathodes depending on the GDL applications. After the application of each GDL, the cathodes were dried and weighted to determine the amount of PTFE added. The total amount of PTFE added for GDL-1, GDL-2, GDL-3 and GDL-4 were (g) 0.26, 0.34, 0.40, and 0.46, respectively. The final porosity of the GDL layer of our cathodes was the result of the porosity of the carbon cloth itself and the pores (channels through the PTFE layers and the carbon cloth) formed during the drying of the PTFE (formation of cracks, retained air bubbles, etc.). Therefore, no specific procedure was used to obtain a given porosity, but it depended on the number of PTFE layers being deposited, the porosity of the carbon support, the adaptation of the successive layers to its morphology and the deposition technique used (brush painting).

Finally, the catalyst layer was deposited following a standard procedure onto the inner side of the cathode to conduct oxygen reduction. The catalyst was prepared by mixing 10% Pt/C (0.5 mg Pt/cm²) and deionized Milli-Q water (Millipore, Billerica, MA, USA) (4.15 μ L/cm²) for 20 seconds. Later, a mixture of Nafion (33.4 μ L/cm²) and 2-propanol (16.7 μ L/cm²) was added to obtain a binding paste. Then, the solution was stirred using a vortex for 20 seconds, adding to the solution between 6 and 8 glass beads. The resulting paste was coated on the side opposite to the diffusion layer coating using a paintbrush. Finally, the coating was air-dried for 24 hours. The cathode was electrically connected by a titanium wire assembled to the carbon cloth support.

An R_{ext} was connected between the cathode and the anode (Figure 1b) to close the electrical circuit. The effect of the number of GDL coating on the AC-MFC performance was studied using replicates with GDL-0 to GDL-4 and under R_{ext} of 10 Ω and 249 Ω .

The anode was inoculated by mixing 14 mL of fresh culture medium and 14 mL of the culture medium from an already working MFC as described by Ribot-Llobet et al.^[42] The culture medium composition contained per L: 15.09 g Na₂HPO₄·2H₂O, 2.06 g KH₂PO₄, 0.2 g NH₄Cl, 4.0 mg FeCl₂, 6.0 mg Na₂S and 5 ml of nutrient

solution, which contained ($\text{g} \cdot \text{L}^{-1}$): 1 EDTA, 0.164 $\text{CoCl}_2 \cdot 6\text{H}_2\text{O}$, 0.228 $\text{CaCl}_2 \cdot 2\text{H}_2\text{O}$, 0.02 H_3BO_3 , 0.04 $\text{Na}_2\text{MoO}_4 \cdot 2\text{H}_2\text{O}$, 0.002 Na_2SeO_3 , 0.02 $\text{Na}_2\text{WO}_4 \cdot 2\text{H}_2\text{O}$, 0.04 $\text{NiCl}_2 \cdot 6\text{H}_2\text{O}$, 2.32 MgCl_2 , 1.18 MgCl_2 , 1.18 $\text{MnCl}_2 \cdot 4\text{H}_2\text{O}$, 0.1 ZnCl_2 , 0.02 $\text{CuSO}_4 \cdot 5\text{H}_2\text{O}$ and 0.02 $\text{AlK}(\text{SO}_4)_2$. Besides, $1.5 \text{ g} \cdot \text{L}^{-1}$ of sodium acetate was added as a substrate. The aqueous solutions were prepared with deionised Milli-Q water (Millipore, Billerica, MA, USA). The initial pH and conductivity were around 7.5 and 13 mS/cm, respectively. All reagents were of analytical grade (Scharlab, Spain).

Analytical Methods and Instrumentation

Acetate was analyzed by gas chromatography (Agilent Technologies, 7820-A) using a flame-ionization detector, DB-FFAB column, and helium as the carrier gas. The cathode surface was assessed by means of SEM using a Jeol JSM 6010 Microscope (JEOL, Ltd, Tokyo, Japan) with integrated EDX probe.^[43] When required, especially for the GDL side, samples were coated with a thin carbon film by thermal evaporation of carbon to avoid misleading charging effects.

The voltage across the R_{ext} (10 or 249 Ω) was monitored by means of a 16-bit data acquisition card (Advantech PCI-1716) connected to a personal computer with the AddControl software developed by the authors in LabWindows/CVI 2017 for data acquisition. The BET technique was used to determine the surface area in each cathode in a Micromeritics ASAP 2000 (N_2) with an accelerated surface area and porosimetry system using nitrogen as adsorption/desorption gas in the Institut de Ciència de Materials de Barcelona (ICMAB, Bellaterra, Spain).

Oxygen Mass Transfer Coefficient of the Cathodes

The oxygen mass transfer coefficient for cathodes with different gas diffusion layers was determined by using a widely reported procedure.^[44,45] The experiments were carried out in abiotic single-chamber AC-MFC. One side of the cathode was in contact with the chamber medium, while the other side was in contact with air (through the GDL). The chamber was filled with deionized water sparged with nitrogen prior to each experiment to remove DO. Then, oxygen was let to naturally diffuse through the cathode from the atmosphere to the reactor while the change in the DO concentration was periodically measured with a DO probe (HI-98193, Hanna Instruments Co., USA) placed in the cell. The overall oxygen mass transfer coefficient (K_L , cm/s) was calculated using equation (3):

$$K_L = \frac{-V}{A \cdot t} \cdot \ln \left(\frac{C_{0c} - C_{0a}}{C_{0c}} \right) \quad (3)$$

where, V is the volume of the chamber (cm^3), A is the projected surface area of the cathode (cm^2), C_{0a} is the DO concentration (g/cm^3) in the reactor chamber at time t (s) and C_{0c} is the DO concentration at equilibrium with the bulk air according to equation (4):

$$C_{0c} = \frac{C_g}{H} \quad (4)$$

Where C_g is the concentration of molecular oxygen in air (mg/L) and H is the dimensionless Henry's coefficient at standard conditions (25°C and 1 atm). A dimensionless H of 31.44 was used as deduced from Sander et al.^[46]

On the other hand, the oxygen diffusion coefficient through each cathode (D_{O} , cm^2/s) was calculated using equation (5) considering the average thickness of each cathode (L_{th}):

$$D_{\text{O}} = K_L \cdot L_{\text{th}} \quad (5)$$

L_{th} was determined as the average of six measurements of each cathode thickness, which were obtained with a digital calliper (CD-6 ASX, Mitutoyo).

Electrochemical Techniques

These techniques were tested in a set of different abiotic cathodes to study the performance of the cell, and specifically that of the cathodes, regardless of the activity of the microorganisms grown in the anode. The electrochemical techniques were systematically applied in a single methacrylate cell using the same bioanode every time that a cathode was replaced by a new one with a different number of GDL coatings.

Electrochemical Impedance Spectroscopy: EIS measurement of an individual electrode (bioanode or cathode) provides useful information about the electrode performance.^[47,48] EIS experiments were completed using an Autolab PGSTAT302 N potentiostat/galvanostat (Methrom Inc.) equipped with a frequency analyzer. Since the aim was to analyze the cathode behavior, EIS measurements were performed using a three-electrode configuration, where the cathode was used as a working electrode, the anode as a counter electrode, and an Ag/AgCl reference electrode (BioLogic) located near the cathode that was used as the reference electrode. EIS tests were carried out under open circuit potential in a frequency range from 100 kHz to 10 mHz. To prevent biofilm detachment and to reduce disturbances of steady-state conditions of the cell,^[49] the amplitude was fixed to 1 mV in AC. The AC-MFC cell was left overnight until organic matter depletion before the EIS experiment. After that, a certain concentration of substrate was added, and the MFC was purged with nitrogen for 30 min.

The equivalent circuit model approach that was used to analyze the experimental results of the electrode (cathode) consisted of a parallel resistor and a constant phase element (CPE), and a series resistor (membrane + solution resistance). In the electrodes, the resistance is related to charge transfer between the electrode and surrounding electrolyte/bacteria. The electrical double layer capacitance is represented by a CPE. The CPE accounts for non-idealities in capacitance such as non-parallel plates, charge leakage, or a nonplanar surface. The resistor between the electrodes accounts for a lumped solution transport resistance through the anode solution, polymer electrolyte membrane (PEM), and cathode liquid film between the electrode and the PEM.

Polarization Curves: The performance of AC-MFC in terms of R_{int} and maximum power output (P_{max}) was assessed through polarization curves. Polarization curves were obtained with a multi-resistance board, which allowed changing the R_{ext} of the cell in the range of 25 Ω to 470 k Ω . Before the polarization, the MFC cell was left to reach steady-state conditions by leaving it 30 minutes under an open circuit (OC). Fresh culture medium was added to ensure substrate availability during the experiments. After that, the polarization curve was performed by changing the resistances from the highest to the lowest one. A 10 minutes period was used for voltage stabilization between each resistance.

Cyclic Voltammetry: The electroactive surface was assessed through CV, using an Autolab PGSTAT302 N potentiostat/galvanostat (Methrom Inc.) equipped with a frequency analyzer. CV measurements were performed using the three-electrode config-

uration used for EIS tests. The electrolyte was 0.01 M $K_4Fe(CN)_6$, 0.01 M $K_3Fe(CN)_6$ and 0.1 M KCl solution. The oxidation of ferrocyanide on the working electrode surface (equation 6) created peaks current of the reduction and oxidation



The current was proportional to the electroactive surface area of the working electrode according to the Randles-Ševčík equation:^[50]

$$I_p = 268600 \cdot n^{3/2} \cdot A \cdot D^{1/2} \cdot C \cdot v^{1/2} \quad (7)$$

Where I_p (A) was the peak current, n was the number of electrons transferred in the redox reaction, A (cm^2) was the electroactive surface area, D ($6.4 \cdot 10^{-6} cm^2/s$) was the diffusion coefficient of $Fe(CN)_6^{-3}$, C (mol/cm^3) was the concentration of the reaction species in the electrolyte and v (V/s) was the scan rate, which was, in these experiments, 0.005 V/s.

Coulombic Efficiency: The coulombic efficiency (CE) was calculated according to equation (8):

$$CE = \frac{\int_{t_0}^{t_f} I dt}{F \cdot b_s \cdot V_L \cdot \Delta C \cdot M_s^{-1}} \quad (8)$$

where t_0 and t_f (s) are the initial and final time of the batch experiment, I (A) is the current, F ($96485 C \cdot mol^{-1} \cdot e^{-1}$) is the Faraday's constant, b_s is the number of electrons transferred in the reaction per mole of substrate, V_L (L) is the volume of the reactor, ΔC ($g \cdot L^{-1}$) is the substrate concentration change over a batch cycle and M_s ($g \cdot mol^{-1}$) is the molecular weight of the substrate.

Acknowledgements

This work was supported by the Spanish Ministerio de Economía y Competitividad (CTQ2017-82404-R) with funds from the Fondo Europeo de Desarrollo Regional (FEDER). Pilar Sánchez Peña is grateful to the FI predoctoral scholarship (2018FI_B01161) from the Catalan Government (Agencia de Gestió d'Ajuts Universitaris i de Recerca). All authors except Jesús Rodríguez are members of the GENOCOV research group (Grup de Recerca Consolidat de la Generalitat de Catalunya, 2017 SGR 1175, www.genocov.com).

Conflict of Interest

The authors declare no conflict of interest.

Keywords: air-cathode · external resistance · gas diffusion layer · microbial fuel cells · thickness

- [1] T. J.-P. Ivase, B. B. Nyakuma, O. Oladokun, P. T. Abu, M. N. Hassan, *Environ. Prog. Sustain. Energy* **2020**, *39*, 13298.
- [2] C. Feng, F. Li, H. Liu, X. Lang, S. Fan, *Electrochim. Acta* **2010**, *55*, 2048–2054.
- [3] B. E. Logan, *Appl. Microbiol. Biotechnol.* **2010**, *85*, 1665–1671.
- [4] M. Ghasemi, W. R. Wan Daud, M. Ismail, M. Rahimnejad, A. F. Ismail, J. X. Leong, M. Miskan, K. Ben Liew, in *Int. J. Hydrogen Energy*, **2013**, pp. 5480–5484.

- [5] G. Antonopoulou, K. Stamatelatou, S. Bebelis, G. Lyberatos, *Biochem. Eng. J.* **2010**, *50*, 10–15.
- [6] E. D'enginyeria, Y. R. Franco, A. Guisasaola, C. Juan, A. B. Labat, *Scale-up Opportunities of Microbial Electrolysis Cells for Hydrogen Production from Wastewater*, n.d.
- [7] A. K. Manohar, F. Mansfeld, *Electrochim. Acta* **2009**, *54*, 1664–1670.
- [8] B. Min, Ó. B. Román, I. Angelidaki, *Biotechnol. Lett.* **2008**, *30*, 1213–1218.
- [9] G. Hernández-Flores, H. M. Poggi-Varaldo, O. Solorza-Feria, M. T. P. Noyola, T. Romero-Castanón, N. Rinderknecht-Seijas, *J. New Mater. Electrochem. Syst.* **2015**, *18*, 121–129.
- [10] G. #4, P. Mcaveney, B. Pedersen, J.-C. Wong, *Microbial Fuel Cell Using Inexpensive Materials*, n.d.
- [11] W. Yang, K. Y. Kim, P. E. Saikaly, B. E. Logan, *Energy Environ. Sci.* **2017**, *10*, 1025–1033.
- [12] D. Pant, G. Van Bogaert, C. Porto-Carrero, L. Diels, K. Vanbroekhoven, *Water Sci. Technol.* **2011**, *63*, 2457–2461.
- [13] A. Chianese, L. Di Palma, E. Petrucci, M. Stoller, J. Rodríguez, N. Rojas, M. Sánchez-Molina, L. González Rodríguez, R. Campana, L. R. Centro Nacional Del Hidrógeno, P. Fernando El Santo, in *Chem. Eng. Trans.* **2016**.
- [14] Z. Wang, G. D. Mahadevan, Y. Wu, F. Zhao, *J. Power Sources* **2017**, *356*, 245–255.
- [15] C. Santoro, A. Serov, K. Artyushkova, P. Atanassov, *Curr. Opin. Electrochem.* **2020**, *23*, 106–113.
- [16] H. Hiegemann, T. Littfinski, S. Krimmler, M. Lübken, D. Klein, K. G. Schmelz, K. Ooms, D. Pant, M. Wichern, *Bioresour. Technol.* **2019**, *294*, 122227.
- [17] R. Flückiger, S. A. Freunberger, D. Kramer, A. Wokaun, G. G. Scherer, F. N. Büchi, *Electrochim. Acta* **2008**, *54*, 551–559.
- [18] S. Cheng, H. Liu, B. E. Logan, *Electrochem. Commun.* **2006**, *8*, 489–494.
- [19] F. Zhang, D. Pant, B. E. Logan, *Biosens. Bioelectron.* **2011**, *30*, 49–55.
- [20] C. Santoro, A. Agrios, U. Pasaogullari, B. Li, *Int. J. Hydrogen Energy* **2011**, *36*, 13096–13104.
- [21] J. Middaugh, S. Cheng, W. Liu, R. Wagner, *How to Make Cathodes with a Diffusion Layer for Single-Chamber Microbial Fuel Cells*, **2008**.
- [22] S. Cheng, B. E. Logan, *Bioresour. Technol.* **2011**, *102*, 4468–4473.
- [23] X. Li, X. Wang, Y. Zhang, N. Gao, D. Li, Q. Zhou, *Int. J. Electrochem. Sci.* **2015**, *10*, 5086–5100.
- [24] L. Birry, P. Mehta, F. Jaouen, J. P. Dodelet, S. R. Guiot, B. Tartakovsky, *Electrochim. Acta* **2011**, *56*, 1505–1511.
- [25] H.-S. Lee, C. I. Torres, P. Parameswaran, B. E. Rittmann, *Environ. Sci. Technol.* **2009**, *43*, 7971–7976.
- [26] K.-J. Chae, M.-J. Choi, K.-Y. Kim, F. F. Ajayi, I.-S. Chang, I. S. Kim, *Environ. Sci. Technol.* **2009**, *43*, 9525–9530.
- [27] P. Zhang, X.-H. Liu, K.-X. Li, Z.-Q. Song, *J. Electrochem. Soc.* **2015**, *162*, F1347–F1355.
- [28] R. Rossi, W. Yang, E. Zikmund, D. Pant, B. E. Logan, *Bioresour. Technol.* **2018**, *265*, 200–206.
- [29] M. Sharma, S. Bajracharya, S. Gildemyn, S. A. Patil, Y. Alvarez-Gallego, D. Pant, K. Rabaey, X. Dominguez-Benetton, *Electrochim. Acta* **2014**, *140*, 191–208.
- [30] S. Srikanth, D. Pant, X. Dominguez-Benetton, I. Genné, K. Vanbroekhoven, P. Vermeiren, Y. Alvarez-Gallego, *Mater.* **2016**, *9*, 601.
- [31] S. Venkata Mohan, R. Saravanan, S. V. Raghavulu, G. Mohanakrishna, P. N. Sarma, *Bioresour. Technol.* **2008**, *99*, 596–603.
- [32] P. C. Nien, C. Y. Lee, K. C. Ho, S. S. Adav, L. Liu, A. Wang, N. Ren, D. J. Lee, *Bioresour. Technol.* **2011**, *102*, 4742–4746.
- [33] X. Zhu, J. C. Tokash, Y. Hong, B. E. Logan, *Bioelectrochemistry* **2013**, *90*, 30–35.
- [34] V. J. Watson, B. E. Logan, *Electrochem. Commun.* **2011**, *13*, 54–56.
- [35] A. E. Tugtas, P. Cavdar, B. Calli, *Bioresour. Technol.* **2011**, *102*, 10425–10430.
- [36] W. Yang, J. Li, Q. Fu, L. Zhang, X. Zhu, Q. Liao, *Bioresour. Technol.* **2017**, *241*, 325–331.
- [37] X. Wang, C. Santoro, P. Cristiani, G. Squadrito, Y. Lei, A. George Agrios, U. Pasaogullari, B. Li, *J. Electrochem. Soc.* **2013**, *160*, G3117–G3122.
- [38] J. Muñoz, R. Montes, M. Baeza, *TrAC Trends Anal. Chem.* **2017**, *97*, 201–215.
- [39] H. Liu, B. E. Logan, *Environ. Sci. Technol.* **2004**, *38*, 4040–4046.
- [40] Y. Feng, Q. Yang, X. Wang, B. E. Logan, *J. Power Sources* **2010**, *195*, 1841–1844.
- [41] J. Middaugh, *How to Make Cathodes with a Diffusion Layer for Single-Chamber Microbial Fuel Cells*, **2008**.
- [42] E. Ribot-Llobet, N. N. Montpart, Y. Ruiz-Franco, L. Rago, J. Lafuente, J. A. Baeza, A. Guisasaola, F. J. Lafuente, *J. Chem. Technol. Biotechnol.* **2014**, *89*, 1727–1732.

- [43] J. Rodríguez, L. Mais, R. Campana, L. Piroddi, M. Mascia, J. Gorauskis, A. Vacca, S. Palmas, *Int. J. Hydrogen Energy* **2021**, DOI 10.1016/j.ijhydene.2021.01.066.
- [44] A. N. Ghadge, M. M. Ghangrekar, *Electrochim. Acta* **2015**, *166*, 320–328.
- [45] S. Kondaveeti, J. Lee, R. Kakarla, H. S. Kim, B. Min, *Electrochim. Acta* **2014**, *132*, 434–440.
- [46] R. Sander, *Atmos. Chem. Phys.* **2015**, *15*, 4399–4981.
- [47] Z. He, F. Mansfeld, *Energy Environ. Sci.* **2009**, *2*, 215–219.
- [48] A. K. Manohar, O. Bretschger, K. H. Nealsen, F. Mansfeld, *Electrochim. Acta* **2008**, *53*, 3508–3513.
- [49] A. P. Borole, D. Aaron, C. Y. Hamilton, C. Tsouris, *Environ. Sci. Technol.* **2010**, *44*, 2740–2745.
- [50] P. Zhu, Y. Zhao, *Mater. Chem. Phys.* **2019**, *233*, 60–67.

Manuscript received: July 4, 2021
Revised manuscript received: August 10, 2021
Accepted manuscript online: August 14, 2021